American Mineralogist, Volume 87, pages 630–641, 2002

Effect of Fe oxidation state on the IR spectra of Garfield nontronite

CLAIRE-ISABELLE FIALIPS, DONGFANG HUO, LAIBIN YAN, JUN WU, AND JOSEPH W. STUCKI*

Department of Natural Resources and Environmental Sciences, University of Illinois, 1102 South Goodwin Avenue, Urbana, Illinois 61801, U.S.A.

ABSTRACT

The effects of Fe oxidation state on the infrared (IR) spectra of dioctahedral smectite were studied using a purified and Na^+-saturated fraction of the Garfield nontronite reference clay. The nontronite was first reduced with sodium dithionite for a period of 10 to 240 min to obtain various Fe reduction levels. The reduced samples were then reoxidized by bubbling O_2 through the suspensions for 8 to12 h. IR spectra were collected on the initially unaltered, the reduced, and the reduced-reoxidized samples. After reduction, changes were observed in the spectral regions of O-H stretching, O-H deformation, and Si-O stretching, indicating that the clay structure was significantly modified beyond merely a change in Fe oxidation state. Furthermore, a new component band in the O-H stretching region of the reduced samples exhibited a pleochroic effect, indicating the possible existence of trioctahedral domains. A large (up to 43 cm^{-1}) downward shift of the main Si-O stretching band of the reduced samples was also observed. Such a large shift indicates that the change in Fe oxidation state in the octahedral sheet strongly affects the structural properties of the tetrahedral sheet, which might further affect physical and chemical properties of the mineral surface. The spectral differences across all three studied regions between unaltered and reoxidized samples after up to 240 min of reduction indicated that the redox process involving sodium dithionite is in some respects irreversible, even though virtually all structural Fe^{2+} can be reoxidized.

INTRODUCTION

Several infrared studies were conducted in the past on Fe reduction in nontronite and Fe-bearing smectites (Roth et al. 1969; Roth and Tullock 1973; Rozenson and Heller-Kallai 1976a, 1976b; Stucki and Roth 1976, 1977; Russell et al. 1979; Komadel et al. 1995; Yan and Stucki 1999, 2000; Manceau et al. 2000b). Their objectives were primarily focused on one of the following research fields: (1) the extent of Fe reduction determined using different reducing reagents, including sodium dithionite, sodium sulfide, anhydrous hydrazine, and aqueous hydrazine; (2) the extent and ease of Fe reduction determined using different kinds of minerals; and (3) the mechanisms involved in the processes of Fe reduction and reoxidation.

Rozenson and Heller-Kallai (1976a, 1976b) concluded that Fe in smectite having both Al and Fe in the octahedral sheet was more easily reduced than Fe in nontronite having Fe as the dominant cation. Russell et al. (1979) suggested that Fe in the tetrahedral sheets was more easily reduced than Fe in the octahedral sheet. Rozenson and Heller-Kallai (1976a, 1976b) proposed that the loss of hydroxyl during reduction occurred through protonation of a single hydroxyl group. Stucki and Roth (1977), however, hypothesized that simultaneous loss of two hydroxyls occurred during reduction and each Fe remaining in the reduced nontronite became fivefold coordinated. Reoxidation restored the lost hydroxyls. The isotope tritium (^3H) was used as a tracer for the measurement of structural OH groups during the redox process and tended to support this hypothesis (Lear and Stucki 1985), but Manceau et al. (2000b) found that structural Fe in reduced nontronite remains sixfold coordinated.

A thorough review of the previous studies revealed several inadequacies in the experiments and conclusions. For example, Rozenson and Heller-Kallai (1976a, 1976b) and Russell et al. (1979) used no buffer in their reduction medium. When sodium dithionite is dissolved in H_2O, the pH drops and causes some dissolution of the clay. So, results showing structural changes reported in those studies may have been confounded by the acid dissolution. Controlling the pH at near neutral or slightly basic minimizes or eliminates this problem.

Furthermore, the reduced samples were often left unprotected from reoxidation (Roth et al. 1969; Roth and Tullock 1973; Rozenson and Heller-Kallai 1976a, 1976b; Russell et al. 1979). The fact is reoxidation readily occurs after reduction if no protection from O_2 is provided. Stucki and co-workers observed that the reduced Na-smectite suspensions are still prone to reoxidation even with very good protection (Stucki, unpublished results).

Another limitation in the previous studies was that the level of reduction was usually less than 50% of the total Fe. Hydrazine can only reduce Fe-rich smectite up to about 10% (Rozenson and Heller-Kallai 1976a, 1976b; Stucki et al. 1996). So, the results obtained using hydrazine are limited. Actually, other inorganic reducing agents are similarly limited, except sodium dithionite (Stucki et al. 1996).

For the last two decades, one focus of Stucki and co-workers

* E-mail: jstucki@uiuc.edu

0003-004X/02/0506–630$05.00

has been to improve the Fe reduction levels and to effectively protect the reduced sample from reoxidation during the experiment by using septum-sealed reaction tubes, an inert-gas atmosphere glove box, and an O_2-free washing apparatus (Stucki et al. 1984a; Komadel et al. 1990; Yan and Stucki 1999; Stucki et al. 2000). The important benefits of these improvements are that the conditions for handling reduced samples are optimized and that the level of reduction is increased to nearly 100% by introducing an inert-gas vent into the reduction reaction tube that allows gaseous reaction products, such as H_2S, to escape and thereby drive the reaction to completion (Komadel et al. 1990).

Few studies have examined the reoxidation of the reduced samples (Stucki and Roth 1977; Komadel et al. 1990, 1995; Yan and Stucki 1999, 2000). However, such studies are very important as they establish the extent of reversibility associated with redox cycles, and thus to direct the application of Fe-bearing clay minerals.

The aim of the present work was to study by IR spectroscopy the reduction of an Fe-rich smectite (Garfield nontronite) at various levels (different ratios of Fe^{2+} to total Fe), and its subsequent reoxidation. Three different regions of the IR spectrum are particularly relevant, namely, O-H stretching, O-H deformation, and Si-O stretching. Results will contribute to the understanding of the reduction and reoxidation processes and of changes in surface properties when Fe-bearing minerals are subject to redox conditions.

Materials and methods

Clay preparation

The clay used in this study was the Garfield, Washington, reference nontronite (API No. 33-a, Ward's Natural Science Establishment, Rochester, NY). The X-ray diffraction (XRD) pattern (not shown) of this initial material prepared according to Stucki et al. (1984a) indicated the presence of a small amount of silica and Fe oxides (i.e., goethite and maghemite; Huo 1997). Because these ancillary phases could complicate the IR spectra, the first step of the present study was to purify the clay. Conventional clay fractionation by sedimentation or centrifugation (Jackson 1979) proved to be insufficient to remove these phases (Huo 1997). Thus, a new method effective for the removal of fine-grained silica and Fe oxides was used (R. Glaser and A. Manceau, personal communication) as follows.

Step 1: A 50 g sample of clay was shaken vigorously in ~500 mL of 1 *M* NaCl solution for 10 h.

Step 2: The sample was centrifuged at 12 000 *g* (Dupont Model Sorvall RC 5C plus centrifuge with SS-34 rotor, 10 000 rpm) and the supernatant liquid replaced with fresh 1 *M* NaCl solution, then shaken again.

Step 3: Steps 1 and 2 were repeated 6 to 7 times and the sample was washed several times with pure H_2O to eliminate excess NaCl and to disperse layers (layers were flocculated at high ionic strength in the presence of NaCl). The first washings in this step consisted of a rapid, short agitation followed by short centrifugation (12 000 *g*), which removed the largest Fe oxide particles that had settled to the bottom of the centrifuge tubes. As the number of washing cycles increased, the layers became more dispersed, resulting in a suspension or stable gel that still contained some impurities. Any brownish-yellow deposit was removed, and then the gel was separated, diluted in pure H_2O, and shaken vigorously to redisperse the layers. The centrifugation speed was increased progressively with the number of dispersion-centrifugation cycles, beginning at 10 000 rpm and ending at 15 000 rpm. The dispersion-centrifugation cycles were continued until no brownish-yellow deposit was observed.

Step 4: The gel was then diluted with 1 *M* NaCl to obtain a concentrated suspension, then excess salts were removed by centrifuge washing and the resulting salt-free suspension was freeze dried for storage.

The final purified sample was greenish in color. Its XRD pattern was typical of dioctahedral smectite without admixed crystalline Fe oxide and quartz, and its structural formula, calculated from chemical analysis, was: $Na_{0.81}(Si_{7.22}Al_{0.78})(Fe^{3+}_{3.64}Fe^{2+}_{0.01}Al_{0.32}Mg_{0.04})O_{20}(OH)_4$ (Manceau et al. 2000a).

Structural Fe reduction and reoxidation

A measured amount of sample (30–50 mg) was dispersed in 20 mL of deionized water in an inert-atmosphere reaction vessel (Stucki et al. 1984a). Ten milliliters of a previously prepared buffer solution [2 parts of 1.2 *M* sodium citrate ($Na_3C_6H_5O_7{\cdot}2H_2O$) and 1 part of 1 *M* sodium bicarbonate ($NaHCO_3$)] was added quickly, and the temperature within the reaction vessel was raised to 70 °C using a water bath. Reducing agent was added in the ratio of 100 mg of sodium dithionite ($Na_2S_2O_4$) to 30 mg of clay, and four different reduced Fe levels of the nontronite were obtained by setting the reduction period to 10, 30, 60, or 240 min. The reduced samples were washed once using deionized, O_2-free H_2O by centrifugation, then re-dispersed. Reoxidized samples were created by bubbling O_2 gas through selected reduced suspensions from each reduction period for 8–12 h to maximize the level of Fe^{2+} to Fe^{3+} reoxidation.

Reduction levels of the reduced and reoxidized samples

The actual levels of Fe reduction (i.e., atomic ratio Fe^{2+}/total Fe) after 10, 30, 60, and 240 min of dithionite treatment and after reoxidation were obtained using the method of Stucki (1981), as modified by Komadel and Stucki (1988). Briefly, this method consists of determining the Fe^{2+}/total Fe ratio of the mineral by photochemical analysis using 1,10-phenanthroline (phen). The Fe^{2+} concentration was first determined by measuring the $Fe(phen)^{2+}_3$ complex formed during HF-H_2SO_4 digestion of the mineral under red light. Then the total Fe was measured after converting any Fe^{3+} in the digestate to $Fe(phen)^{2+}_3$ by photochemical reduction using a mercury vapor lamp.

Infrared spectroscopy

Data acquisition. IR spectra were recorded in transmission mode, within the 400–4000 cm^{-1} range, with a 1 cm^{-1} resolution, using a Midac M2000 FTIR spectrometer, combined with the Grams/386 program for data acquisition. The spectrometer was constantly purged with vaporized liquid N_2 to avoid H_2O and CO_2 contamination. The IR spectra in the spectral ranges of structural O-H stretching and deformation (i.e., 3000–3800 and 550–950 cm^{-1}, respectively) were collected using self-supporting films. To make comparisons among the spectra, holders with a 15 mm diameter hole were used on every film, the intensity of

each spectrum was normalized to a sample mass of 10 mg/film, and the offset was adjusted for some spectra. The IR spectra in the spectral range of Si-O stretching (i.e., 800–1300 cm^{-1}) were collected using window deposits. The actual size of the window deposit being very difficult to control, no weight normalization was made in this IR range. Instead, the maximum absorption intensity of each spectrum was normalized to an arbitrarily chosen value to allow an easy comparison of the positions of the Si-O bands.

Preparation and handling of clay films. The self-supporting films were made from 4–13 mg of sample using a mini-pressure-plate apparatus with a Millipore membrane filter (Stucki et al. 1984c). The films of the unreduced and reoxidized samples were prepared under ambient conditions, but kept in a desiccator containing P_2O_5 for about 24 h to remove the adsorbed H_2O before data collection. The films of the reduced samples were prepared inside a glove box under an inert gas atmosphere to prevent reoxidation, and were evacuated in the antechamber of the glove box for a few hours to remove excess adsorbed H_2O. Prior to removal from the glove box, the reduced dry films were transferred to a sealed vacuum cell (similar to the one described by Angell and Schaffer 1965) to prevent reoxidation and rehydration. Most of the IR spectra were acquired without removing the clay films from the sealed vacuum cell. But, in some cases, spectra had to be measured by placing the film directly into the sample chamber without protection from the atmosphere, except for the normal dry N_2 purge, because the window material of the vacuum cell (ZnSe) is opaque to IR radiation at wavenumbers lower than 650 cm^{-1}. These measurements were obtained rapidly (<5 min) and a check of the reduction levels after data collection revealed no change.

Preparation of window deposits. Because of the strong absorptivity of Si-O bands, the self-supporting films were too thick to be used for Si-O band measurement. An alternative technique was to deposit and dry about 1 mL of suspension (containing 2 mg of clay) onto a ZnSe polished disk (25 mm in diameter and 2 mm in thickness). The window deposits of the unreduced and reoxidized samples were prepared under ambient conditions. Those of the reduced samples were prepared and dried inside the glove box under an Ar atmosphere, then transferred to a sealed vacuum cell prior to removal from the glove box for IR spectral acquisition.

Deconvolution in the OH-stretching region. IR spectra of the unaltered and reduced samples in the OH–stretching region were deconvoluted using the Grams/32 computing software (version 4.11, Galactic Industries Corporation, Salem, NH). In theory, vibrational bands are Lorentzian, however, various factors (instrumental or compositional) affect their shape, leading to a Gaussian or mixed Gaussian-Lorentzian distribution (Strens 1974). Thus, the IR spectra were fitted using bands of mixed Gaussian-Lorentzian shape. The optimum Gaussian-Lorentzian mixing ratios were automatically determined by the curve-fitting program of Grams/32. The position, band-width, and intensity of each component were generally left variable, but were sometimes constrained within a specific range to obtain a satisfactory fitting as determined by the shape and position of coherent components, a small value for the minimization function χ^2, and good agreement between experimental and calculated profiles.

Results and discussion

Reduction levels of the reduced and reoxidized samples

The reduction levels (Fe^{2+}/total Fe) of the reduced and reduced-reoxidized samples are given in Table 1. As expected, the levels of reduction varied significantly from one experiment to the other, depending in part on differences in reduction time. Hereafter, reduction levels will be identified by reduction period (i.e., 10, 30, 60, or 240 min) instead of by reduction level. Only a small amount of Fe^{2+} was unrestored to Fe^{3+} after reoxidation (Table 1, Fe^{2+}/total Fe ≤0.011).

OH stretching: 3000–3800 cm^{-1} IR region

The characteristic OH-stretching bands of the unaltered (unreduced) and reduced nontronite samples fall in the range 3500 to 3650 cm^{-1} (Fig. 1), which overlaps the symmetrical and asymmetrical H_2O-stretching bands (Farmer 1974). For the initially unaltered mineral (reduction time = 0), the OH band is relatively sharp and centered at 3570 cm^{-1} at maximum intensity. This position is typical for dioctahedral Fe-bearing smectites with $(Fe^{3+})_2OH$ being the predominant OH environment (Goodman et al. 1976; Russell et al. 1979). However, the shoulder at 3530 cm^{-1} is of uncertain origin.

To understand better the shape of the IR spectrum of the unaltered Garfield nontronite, the spectrum was deconvolved

Table 1. Reduction levels (i.e., measured atomic ratio Fe^{2+}/total Fe) of the reduced and reoxidized Garfield nontronite

Reduction time	10 min	30 min	60 min	240 min
Reduced Garfield	20 ± 5%	40 ± 5%	65 ± 5%	~100%
Reoxidized Garfield	0.5 ± 0.2%	0.7 ± 0.2%	0.8 ± 0.2%	1.1 ± 0.2%

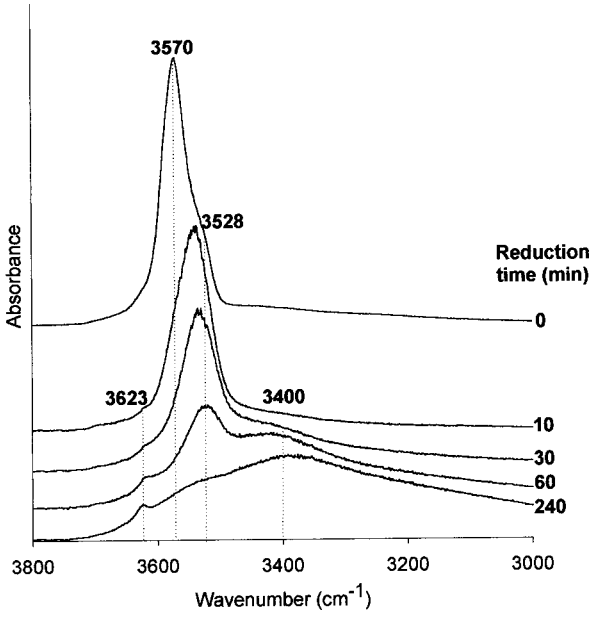

Figure 1. Normalized infrared spectra in the OH-stretching region of the initially unaltered Garfield nontronite and of the samples reduced during 10 to 240 min with buffered sodium dithionite.

into several component bands. To obtain a satisfactory fit of the experimental spectrum, two water bands near 3490 and 3285 cm^{-1} were required; the position, intensity, and attribution of these water bands will be discussed later. The cationic composition of the unaltered Garfield nontronite octahedral sheet (3.64 Fe, 0.32 Al, and 0.04 Mg) implies the presence of at least 3 different OH-stretching bands due to FeFeOH, FeAlOH, and FeMgOH environments. However, a better fit was obtained using 5 OH bands. Figure 2 illustrates one coherent deconvolution with a small χ^2 value (2.2) and a good agreement between experimental and calculated profiles ($R^2 = 0.9978$). The integrated area of each OH-stretching component was normalized to the total area of all components. The position, normalized integrated area, and assignment of the respective OH-stretching bands are presented in Table 2. If the absorption coefficients of all the OH vibrators are equal, then the relative integrated area of each OH band corresponds to the actual proportion of the corresponding OH environment.

No satisfactory fit was possible without a small component band at ~3638 cm^{-1} (1 in Fig. 2), which is attributed to an AlAlOH environment. Its relative area compared to the AlFeOH band (located at 3607 cm^{-1}, 2 in Fig. 2) indicates that up to ~20% of ^{VI}Al may be paired with another ^{VI}Al.

The ~3530 cm^{-1} shoulder is generated by a relatively intense band located at 3532 cm^{-1} (5 in Fig. 2). Several assignments for this band can be proposed based on its position, but its relative intensity is less easily explained. The presence of $Fe^{3+}Fe^{2+}OH$ or $(Fe^{2+})_2OH$ environments would generate IR bands in this range (Stubican and Roy 1961b), but this assignment is impossible for the unaltered Garfield nontronite as it contains virtually no Fe^{2+}. Likewise, this band is too intense and narrow to be attributed to water.

Several alternative assignments can be proposed. First, this band could be due to *cis*-vacant, *trans*-occupied $(Fe^{3+})_2OH$ clusters ($Fe^{3+}_{cis}Fe^{3+}_{trans}\square_{cis}OH$) as suggested by Lear and Stucki (1990). The band position for this grouping would be at lower energy than the *trans*-vacant situation because, in the latter, the two OH dipoles lie close to the plane of the layers but are pointing toward each other, generating stronger OH bonds, due to proton-proton repulsion. In the *cis*-vacant case, little interaction occurs between the two OH dipoles because they are in different planes and are oriented toward the vacant octahedral site; hence the OH bond is weaker. The $Fe^{3+}_{cis}Fe^{3+}_{trans}\square_{cis}OH$ band should, therefore, be at lower wavenumber than the $(Fe^{3+}_{cis})_2\square_{trans}OH$ band, which is consistent with the observed peak positions.

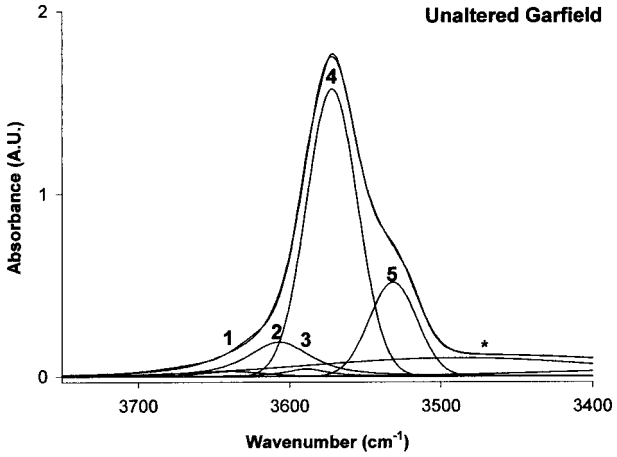

FIGURE 2. Deconvolution of the unaltered Garfield nontronite IR spectrum into several components (1–5, Table 2) in the OH-stretching range; experimental and calculated curves (* = band attributed to water).

The large relative area of the 3532 cm^{-1} band is, however, more difficult to rationalize by the *cis*-vacant scenario. Its intensity is almost one-third of the 3572 cm^{-1} band (4 in Fig. 2), but the probability of the fraction of *cis*-vacant sites being that large is extremely remote. Manceau et al. (2000a) reported that, based on XRD evidence, the fraction of *cis*-vacant sites is limited to less than 5% of the total sites, but Lear and Stucki (1990) proposed a fraction as high as 13%. At these levels, the observed relative intensities would require the O-H absorption coefficient for the $Fe^{3+}_{cis}Fe^{3+}_{trans}\square_{cis}OH$ configuration to be at least double that of the $(Fe^{3+}_{cis})_2\square_{trans}OH$ configuration.

Another possible assignment for the 3532 cm^{-1} band could be to $(Fe^{3+})_2OH$ with the OH group pointing toward the apical oxygen of an Al tetrahedron ($Fe^{3+}_2O\text{-}H\cdots O_T\text{–}^{IV}Al$). The substitution of Al^{3+} for Si^{4+} in a tetrahedron generates a local negative charge on its apical oxygen (O_T). If one of the two tetrahedra directly adjacent to an octahedral vacancy is occupied by Al, the proton of the nearest OH dipole will be attracted toward its O_T, changing the orientation of the OH group and thus weakening the OH bond. Therefore, we expect the $(Fe^{3+})_2O\text{-}H\cdots O_T\text{–}^{IV}Al$ band to be at lower wavenumber than 3572 cm^{-1}. Only ~10% of the tetrahedra in the Garfield nontronite are occupied by Al, but the relative area of the 3532 cm^{-1} and 3572 cm^{-1} bands are 23.5 and 76.5%, respectively. Thus, if we hypothesize that all the ^{IV}Al are selectively distributed in tetrahedra toward which the OH dipoles are pointing, then the relative area of the $(Fe^{3+})_2O\text{-}H\cdots O_T\text{–}^{IV}Al$ band would be 23.5% only if the absorptivity were 2.7 times larger than when the OH is pointing toward two Si tetrahedra. The length and orientation of the OH bond when pointing toward the O_T of an Al tetrahedron would give a larger projection on the $\vec{a}\text{–}\vec{b}$ plane than when the two adjacent tetrahedra are occupied by Si. Therefore, we would expect the absorptivity coefficient of the 3532 cm^{-1} band to be significantly higher than that of the 3572 cm^{-1} band but certainly not as much as 2.7 times. Thus, although we cannot discard this hypothesis, it is insufficient to explain the presence of such an intense 3532 cm^{-1}.

Another explanation for the 3532 cm^{-1} band could be that it arises from a crystal-field effect due to the substitution of ^{IV}Al for ^{IV}Si (Caspers and Buchanan 1962; Farmer and Russell 1964). Caspers and Buchanan (1962) showed that the electrostatic-field effects have a great influence on the OH–stretching vibrations in LiOH, $Ca(OH)_2$, and $Mg(OH)_2$. Random substitutions of ^{IV}Al for ^{IV}Si in the Garfield nontronite could act as structural irregularities and modify the crystal field in the environment of the nearest FeFeOH groupings. This substitution could lead to two different ranges of O-H distances and, thus, two different frequencies. This crystal-field effect also could be responsible for the anomalous antiferromagnetic behavior of the unaltered Garfield nontronite at low temperature (Lear and Stucki 1990).

Further investigations are needed to validate or discard these hypotheses.

The 3532 cm^{-1} band also could be attributed to the symmetric $(Fe^{3+})_2OH$ vibration. Each pair of Fe^{3+} shares two OH groups that are related by a center of symmetry. A coupling between the vibrations of these two OH groups can generate two vibrations: one in which the OH groups are out of phase (antisymmetric vibration located at 3572 cm^{-1}), and the other in which the OH groups are in phase (symmetric vibration). The symmetric vibration should be IR inactive but could generate a weak band around 3630–3650 cm^{-1} if the symmetry of the structure were not ideal (i.e., Farmer and Russell 1964). Although this hypothesis alone cannot explain the intense 3532 cm^{-1} band, it cannot be rejected because of our poor understanding of the structure and symmetry of the Garfield nontronite.

As the reduction time increased from 10 to 60 min (i.e., as more Fe^{3+} in the clay was reduced to Fe^{2+}), the overall OH band shifted progressively downward to 3528 cm^{-1}, its width increased, and its intensity decreased (Fig. 1). After 240 min of reduction, the structural OH band almost disappeared. After 10 min of reduction, a narrow band appeared at ~3623 cm^{-1} and a broad water band was clearly observed at ~3400 cm^{-1}. With the advancement of the reduction process, the 3623 cm^{-1} band increased slightly in intensity while the intensity of the 3400 cm^{-1} band increased greatly.

To understand better the changes occurring in the IR spectrum of the Garfield nontronite with increased reduction time, spectral deconvolution of the reduced samples was attempted. The spectra of the reduced samples were normalized to the total area of all OH-stretching components in the unaltered Garfield nontronite to allow a semi-quantitative approach to understanding band intensities. Each deconvolution was performed using the minimum number of components necessary to obtain a satisfactory fit ($\chi^2 < 25$, $R^2 > 0.99$). Each deconvolution included two broad water bands at 3415–3485 and 3205–3285 cm^{-1}, a

TABLE 2. Position ($\bar{\nu}$), integrated area (A) and attribution of the OH-stretching infrared bands of the unaltered Garfield nontronite

Band	OH environment	$\bar{\nu}$ (cm^{-1})	A (%)
1	AlAlOH	3638	1.69
2	Fe^{3+}AlOH	3607	12.48
3	Fe^{3+}MgOH	3589	2.06
4	$Fe^{3+}Fe^{3+}$OH	3572	64.12
5	$Fe^{3+}Fe^{3+}$OH*	3532	19.65
Total			100.00

* Uncertain assignment, see text.

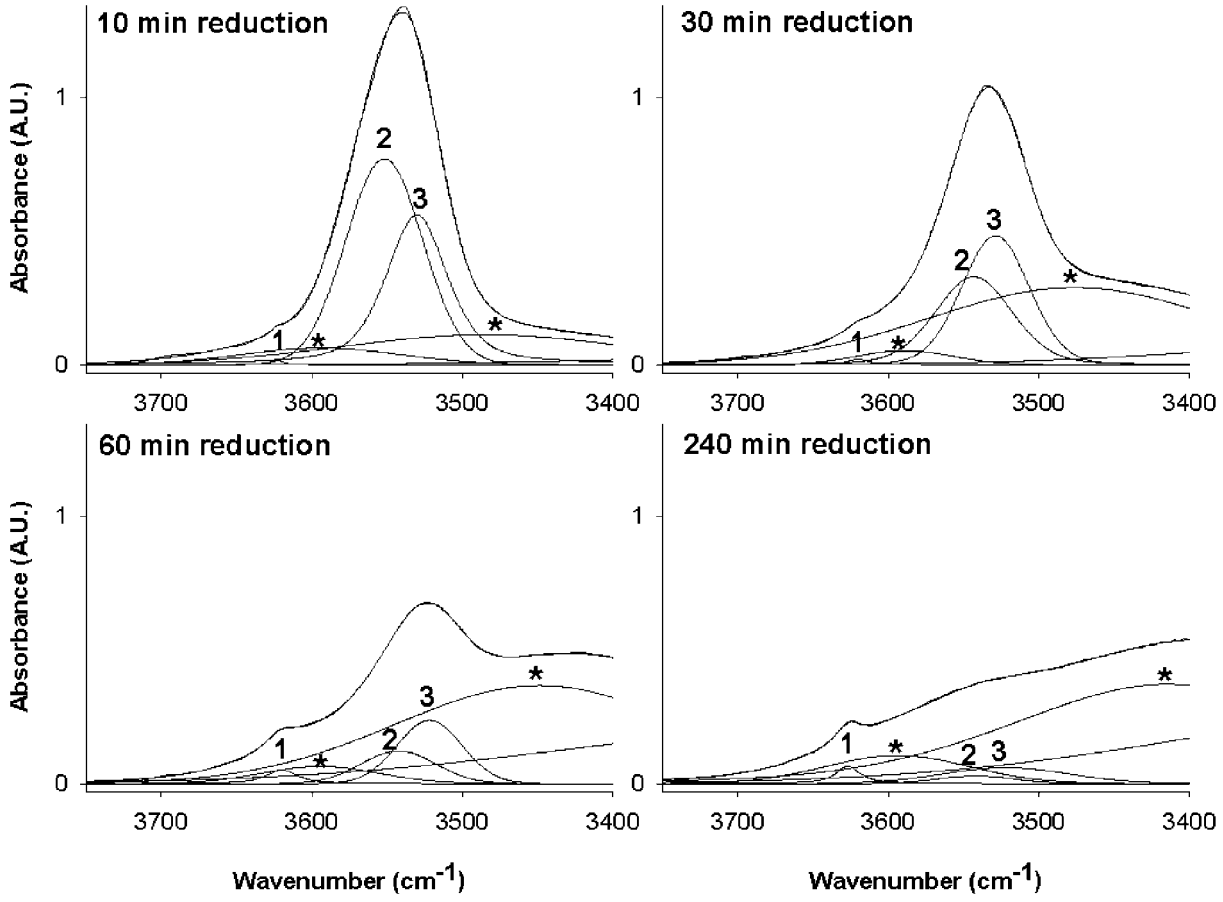

FIGURE 3. Deconvolution of the reduced Garfield nontronite IR spectra into several components (1–3, Table 3) in the OH-stretching range; experimental and calculated curves (* = bands attributed to water).

narrower band at ~3590 cm^{-1} (which may also be attributed to water), and three OH-stretching bands between 3520 and 3630 cm^{-1}. (The position, intensity, and assignment of the water bands will be discussed later.) Results from representative satisfactory deconvolutions are reported in Figure 3 and Table 3.

The 3620–3627 cm^{-1} component (component 1, Fig. 3, Table 3), apparently absent from the unaltered Garfield nontronite (Fig. 2, Table 2), was present in the spectra of each reduced sample and increased in relative area with increasing reduction time (Figs. 1 and 3, Table 3). This trend indicates that a new cationic combination (or distribution) may have emerged after just 10 min of reduction. No absorption near 3620–3627 cm^{-1} has ever been reported for Fe-rich, dioctahedral layer silicates, although Burns and Strens (1966) observed fundamental OH-stretching vibrations of $(Fe^{2+})_3OH$ at 3625 cm^{-1} and 3615 cm^{-1} in two amphibole series (i.e., tremolite-ferroactinolite and cummingtonite-grunerite). Therefore, the 3620–3627 cm^{-1} band of the reduced Garfield nontronite samples may be due to $(Fe^{2+})_3OH$ trioctahedral groupings formed during the sodium dithionite reduction process, as already proposed by Manceau et al. (2000b). This assignment is supported by the pleochroic behavior of this band (Fig. 4), which was detected by comparing the spectra obtained from self-supporting films of the 240 min reduced sample oriented at 90 and 60° to the incident IR beam. Spectra were thickness-normalized to allow a valid comparison between them. The intensity of the 3622 cm^{-1} band increased from the 90 to the 60° orientation. This pleochroic behavior can only be observed in trioctahedral clay minerals and indicates that the OH groups of the reduced sample are oriented perpendicular to the plane of the clay film. Hence, trioctahedral domains must form in certain zones of dioctahedral smectites. Manceau et al. (2000b) showed polarized EXAFS and XRD evidence that, in fact, Fe atoms migrate from *cis*- to neighboring *trans*-positions in the octahedral sheet as the Fe^{2+} content increases, yielding $(Fe^{2+})_3OH$ entities and large cavities. This result clearly is a new concept that needs further investigation and verification, particularly with respect to its structural implications.

TABLE 3. Position $\bar{\nu}$ and relative area (A) of the OH-stretching infrared bands of the 10 to 240 min reduced Garfield nontronite

Band	10 min reduction		30 min reduction		60 min reduction		240 min reduction	
	$\bar{\nu}$(cm^{-1})	A (%)	$\bar{\nu}$(cm^{-1})	A (%)	$\bar{\nu}$(cm^{-1})	A (%)	$\bar{\nu}$(cm^{-1})	A (%)
1	3625	0.25	3620	0.49	3620	1.73	3627	1.79
2	3550	47.21	3543	21.66	3542	7.21	3542	1.74
3	3530	33.55	3529	27.04	3522	12.22	3522	5.97
Total		81.01		49.19		21.15		9.50

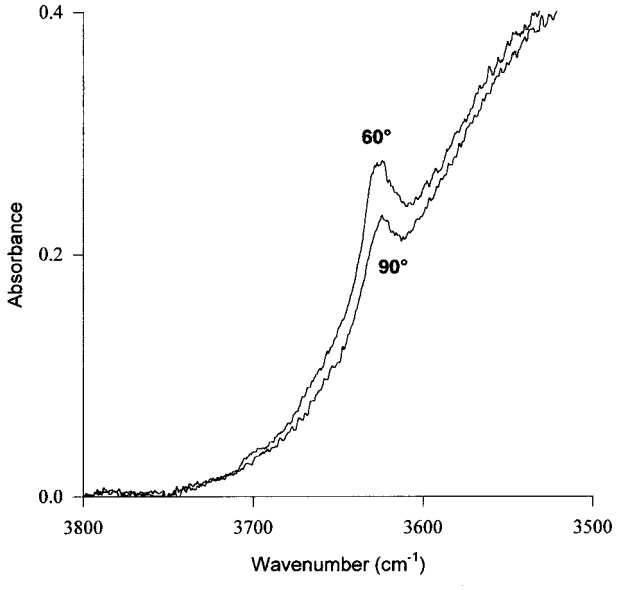

FIGURE 4. Normalized infrared spectra of the 240 min reduced Garfield nontronite film oriented 90 and 60° to the incident beam.

With the increase of reduction time, the total area of the OH-stretching bands decreased progressively from 100% for the unaltered Garfield nontronite (Fig. 2, Table 2) down to 9.5% for the fully reduced sample (Fig. 3, Table 3). This behavior indicates a progressive loss of OH groups during the reduction process. This finding is in agreement with the mechanism of smectites reduction, proposed by Roth and Tullock (1973) and modified by Stucki and Roth (1977), involving the three following reactions:

$$m\ (Fe^{3+})_{structural} + m\ e^- \rightarrow m\ (Fe^{2+})_{structural} \quad (1)$$

$$2n\ [OH^-]_{structural} \rightarrow n\ [O^{2-}]_{structural} + n\ H_2O \quad (2)$$

$$n\ [O^{2-}]_{structural} + n\ [H^+]_{solvent} \rightarrow n\ [OH^-]_{structural}. \quad (3)$$

According to this mechanism, the Garfield nontronite is reduced by an electron transferred from the sodium dithionite (Eq. 1), accompanied by the condensation of structural OH and formation of water (Eq. 2). The structural oxide formed in Equation 2 would then reprotonate (Eq. 3). Thus, a total of *n*/*m* structural OH would be lost for each Fe^{3+} reduced to Fe^{2+}. For the SWa-1 ferruginous smectite, Lear and Stucki (1985) estimated the *n*/*m* ratio to be about 0.32 and to be invariant over the range of Fe^{2+} contents they studied. In the present study, assuming that the unaltered Garfield nontronite contains the theoretical number of OH per formula unit (4 OH), and neglecting any possible difference in the absorption coefficient of all the OH-stretching bands of the unaltered and reduced samples, the estimated *n*/*m* ratio would be about 1.0–1.4 (calculated from Table 3). This large discrepancy with the value estimated by Lear and Stucki (1985) indicates that the absorptivities of the OH vibrators probably decreased during the reduction process, resulting in an overestimation of the number of OH lost, and thus leading to an inaccurate determination of the *n*/*m* ratio from the IR data. Changes in the ^{VI}Fe oxidation level and partial dehydroxylation can effectively generate changes in the orientation of the remaining OH dipoles and thus in their absorptivity. Besides, if the 3620–3627 cm^{-1} band is effectively due to $(Fe^{2+})_3OH$ entities, the OH group is perpendicular to the plane of the clay and the corresponding absorptivity is then smaller than that of FeMOH (with M = Fe, Al, or Mg).

The progressive shift of the overall OH band from 3570

down to 3528 cm^{-1} upon reduction (Fig. 1) reflects a diversification of the OH environment from $(Fe^{3+})_2OH$ to combinations of $(Fe^{3+})_2OH$, $Fe^{3+}Fe^{2+}OH$, and $(Fe^{2+})_2OH$, and variations in the relative fractions of these three cationic groupings. Indeed, increasing the Fe-reduction level produced more $Fe^{3+}Fe^{2+}OH$ and $(Fe^{2+})_2OH$ associations, generating bands at much lower wavenumbers than 3570 cm^{-1}. This result is particularly obvious when comparing the positions and relative areas of components 2 and 3 of the deconvolved spectra of the reduced samples (Fig. 3, Table 3). Component 2, which can be attributed to a mixture of $Fe^{3+}MOH$ (with M = Al or Fe^{3+}) and $Fe^{3+}Fe^{2+}OH$, shifted from 3550 down to 3542 cm^{-1}, indicating a decrease in the proportion of $(Fe^{3+})_2OH$ environments in favor of $Fe^{3+}Fe^{2+}OH$ environments. Component 3, attributed to a mixture of $Fe^{3+}Fe^{2+}OH$ and $(Fe^{2+})_2OH$, shifted from 3530 down to 3522 cm^{-1}, indicating an increase in the proportion of $(Fe^{2+})_2OH$ environments compared to $Fe^{3+}Fe^{2+}OH$ environments. Although the components 2 and 3 both decreased significantly in area with increasing reduction time, due in part to dehydroxylation, the area of component 3 increased relative to component 2. This behavior indicates once more the significant increase in the proportion of $Fe^{3+}Fe^{2+}OH$ and $(Fe^{2+})_2OH$ environments over $Fe^{3+}MOH$ environments.

Analysis of the positions and integrated areas of the water-stretching bands for the unaltered and reduced Garfield nontronite samples (Table 4) revealed that the $\bar{\nu}_1$ band, which is assigned to weakly hydrogen-bonded water (Farmer 1971, 1974), was absent from the unaltered spectrum but is present in the reduced sample. Although its position is relatively constant in the reduced sample, its band area increased progressively from 7.9% in the 10 min reduced sample up to 12.0% for the 240 min fully reduced sample.

The $\bar{\nu}_2$ and $\bar{\nu}_3$ bands were both present in all the spectra and, with increasing reduction time, shifted significantly to lower wavenumbers and increased in intensity. These bands are due to the stretching vibrations of water OH groups involved in hydrogen bonding (Farmer 1971, 1974). Their progressive shift to lower wavenumbers is consistent with the progressive shift of the H-O-H-bending band from 1627 up to 1632 cm^{-1} (present study, data not shown; Yan and Stucki 2000). These shifts of the H-O-H-stretching and bending bands with the increasing Fe reduction indicate that the water molecules become increasingly more strongly hydrogen-bonded to the clay surface or to other water molecules. Furthermore, the total area of the $\bar{\nu}_2$ and $\bar{\nu}_3$ H-O-H–stretching bands increased simultaneously with the decrease in total area of the structural OH-stretching bands as the time of reduction increased from 10 to 240 min, indicating that the loss of structural OH may be coupled to the increase in H-O-H (Fig. 5). We propose that the $\bar{\nu}_2$ and $\bar{\nu}_3$ bands are due to stretching vibrations of strongly hydrogen-bonded H_2O molecules within the crystal structure. These H_2O molecules derive from the dehydroxylation and condensation of structural OH groups during the reduction process (Eq. 2) and could have been trapped within large cavities formed upon the migration of some Fe^{2+} from *cis*- to *trans*-octahedral sites. To explain these phenomena, we propose the following sequence of events. With the increase of reduction time, more Fe^{3+} ions are reduced to Fe^{2+} (Eq. 1), more Fe^{2+} ions migrate from *cis*- to *trans*-sites (formation of the trioctahedral domains), more or larger cavities are formed within the octahedral sheet, more OH groups are lost (Eq. 2), more water molecules condense within the cavities, and these molecules thus become more hydrogen-bonded with the clay surface and/or with each other.

The effect of reoxidation on the H-O-H and structural OH stretching is illustrated by comparing the unaltered, reduced, and reduced-reoxidized samples together (Fig. 6). The greater the initial level of reduction, the less reversible the IR spectra. When the nontronite was reduced for only 10 min, the OH band was essentially restored to its original intensity and wavenumber (3570 cm^{-1}) upon complete reoxidation (Fig. 6a). This result indicates that a change in Fe oxidation state is the primary process during the first 10 min of reduction. Indeed, if any cationic rearrangement had occurred during this period of reduction, the IR spectrum of the reoxidized sample would be at least slightly different from that of the unaltered clay, as complete restoration to the original site occupancy and arrangement would be highly

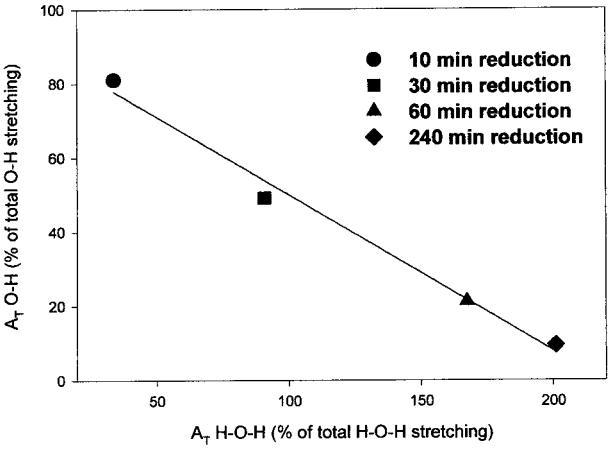

FIGURE 5. Total area of the structural OH-stretching bands vs. the sum of the $\bar{\nu}_2$ and $\bar{\nu}_3$ H-O-H–stretching bands.

TABLE 4. Position ($\bar{\nu}_i$, with i = 1, 2, and 3), relative area (A_i), and total area (A_T) of the H-O-H–stretching infrared bands of the unaltered and reduced Garfield nontronite

Reduction time (min)	Fe^{2+}/Total Fe (%)	$\bar{\nu}_1$ (cm^{-1})	A_1 (%)	$\bar{\nu}_2$ (cm^{-1})	A_2 (%)	$\bar{\nu}_3$ (cm^{-1})	A_3 (%)	A_T (%)
0	0	–	–	3490	24.32	3285	10.75	35.07
10	20	3594	7.92	3485	25.73	3285	8.00	41.65
30	40	3589	3.98	3476	66.85	3268	23.81	94.64
60	65	3594	5.93	3449	84.22	3236	83.10	173.25
240	100	3594	12.00	3415	95.89	3205	105.09	212.98

Note: Each spectrum was normalized to the total area of the OH-stretching bands of the unaltered Garfield.

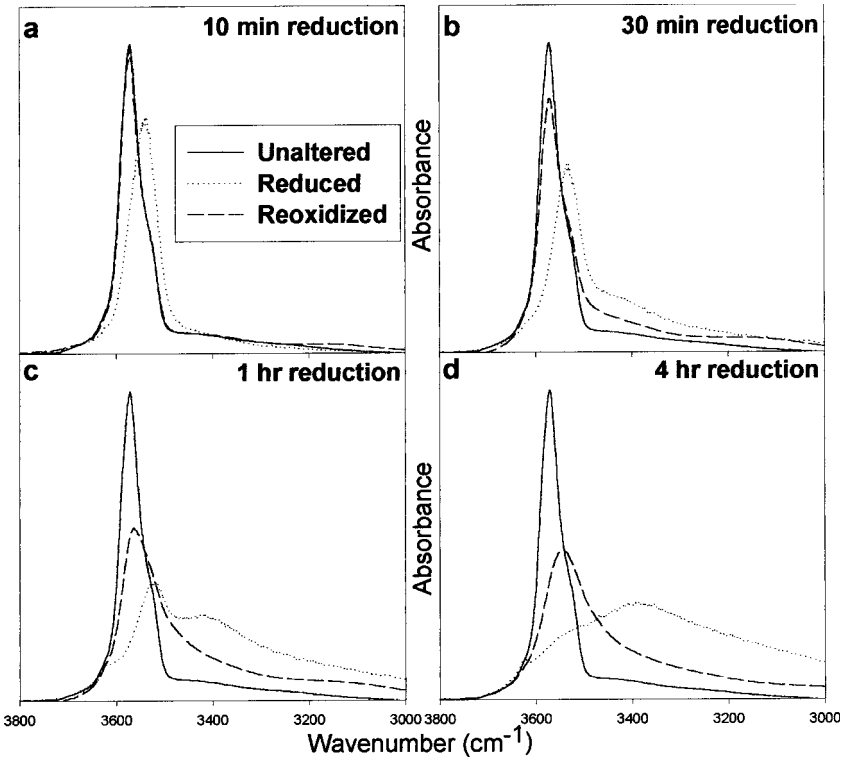

FIGURE 6. Normalized infrared spectra in the OH-stretching region of the Garfield nontronite reduced during different times, then reoxidized: reduction times of (**a**) 10 min; (**b**) 30 min; (**c**) 60 min; and (**d**) 240 min. The spectrum of the initially unaltered Garfield nontronite is given in each plot for comparison.

unlikely. Moreover, the intensity decrease of the OH-stretching band after 10 min of reduction (Figs. 1, 3, and 6a) must be due to a superficial dehydroxylation (on the edge and within the external layers) as it was readily reversed upon reoxidation.

Reoxidation of the 30 min reduced sample restored the OH band to its original wavenumber (3570 cm^{-1}) but its intensity was not restored totally (Fig. 6b). This intensity difference indicates that as the reduction process proceeds, the loss of OH becomes more extensive and less reversible upon reoxidation. Restoration of the peak position, however, shows that during the first 30 min of reduction, no significant cationic rearrangement occurred.

Reoxidation of the 60 and 240 min reduced samples restored neither the peak intensity nor the frequency of the original OH band (Figs. 6c and 6d). Reoxidation shifted the OH band only back to 3563 and 3547 cm^{-1}, respectively. This result suggests that both cationic rearrangements and extensive loss of structural OH groups occurred during the first hour of reduction and that reoxidation failed to restore the unaltered configuration. The loss of OH was only partially restored and the cationic rearrangement in the reoxidized sample was redistributed into a different configuration from the unaltered sample.

Whatever the time of reduction, the 3620–3627 cm^{-1} band previously observed in the spectra of the reduced samples was lost upon reoxidation. If this band was effectively due to $(Fe^{2+})_3OH$ domains generated by the migration of Fe^{2+} from *cis*- to *trans*-sites during reduction, its disappearance after reoxidation indicates that the Fe were redistributed within the octahedral sheet to return to a fully dioctahedral sheet. Either the same Fe ions that had migrated during reduction moved back to their original positions (reversibility; 10 and 30 min reduction), or reoxidation redistributed the cations into a dioctahedral configuration different from that of the unaltered Garfield nontronite (irreversibility; >30 min of reduction).

Interestingly, the tightly bound H_2O band (~3400 cm^{-1}) that was present in the reduced samples (Figs. 1 and 3) was also mainly lost when the samples were reoxidized, suggesting that most of the hydrogen-bonded H_2O was either released to solution or re-incorporated into the structure. This finding is in agreement with the assignment of this band to H_2O molecules trapped inside large cavities created upon reduction by the migration of Fe^{2+} from *cis*- to neighboring *trans*-positions in the octahedral sheet (Manceau et al. 2000b; Drits and Manceau 2000). By redistributing Fe within the octahedral sheet, reoxidation fills the cavities that had formed during reduction, re-incorporating part of the trapped H_2O molecules into the structure and releasing possible extra H_2O to solution.

O-H deformation: 550–950 cm^{-1} IR region

Deformation bands belonging to M-O-H (with M = Mg, Al, or Fe) in the unaltered (unreduced) and reduced samples are shown in Figure 7. No spectral deconvolutions were performed for this region because of the great uncertainty in the baseline. The band located at 822 cm^{-1} is assigned to $(Fe^{3+})_2OH$ deformation (Serratosa 1960; Stubican and Roy 1961b; Farmer and Russell 1964; Farmer 1974). The 870 cm^{-1} band is attributed to deformation modes of $AlFe^{3+}OH$ (Russell et al. 1970; Farmer 1974). The weak 913 cm^{-1} band is attributed to Al_2OH deformation (Farmer and Russell 1964), justifying the use of a weak Al_2OH-stretching band for the deconvolution of the unaltered

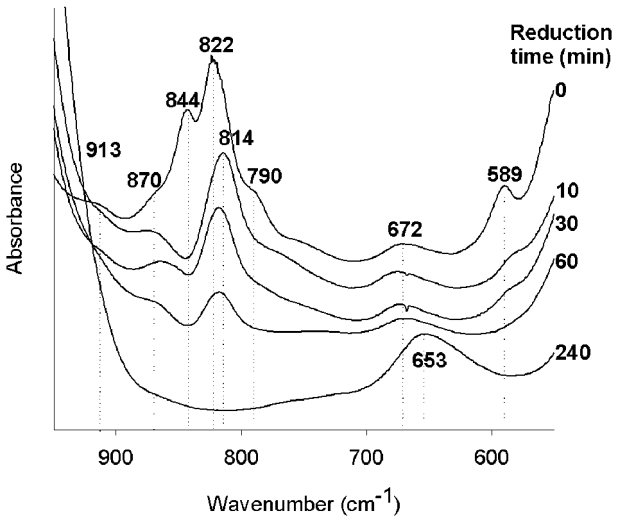

FIGURE 7. Normalized infrared spectra in the OH-deformation region of the initially unaltered Garfield nontronite and of the samples reduced during 10 to 240 min with buffered sodium dithionite.

Garfield nontronite spectrum in the OH-stretching range (Table 2).

The assignment of the 844 cm^{-1} band is still under discussion. Goodman et al. (1976) attributed it to deformation modes of $AlFe^{3+}OH$ where Fe is the principal matrix, noting that this band shifts to 870 cm^{-1} if the neighboring cations are Al. Such an assignment, however, fails to explain the presence of both 870 and 844 cm^{-1} bands simultaneously. Stucki and Roth (1976) assigned the 844 cm^{-1} band to an Fe-(OH)-stretching vibration. But, as already discussed by Russell et al. (1979), Fe-(OH)-stretching would unlikely generate an IR band in this wavenumber range. Russell et al. (1970) and Cracium (1984) observed an AlMgOH-deformation band at 839–848 cm^{-1} in montmorillonite, and such an assignment for the 844 cm^{-1} band of nontronite has been adopted by several authors (i.e., Petit et al. 1992; Grauby et al. 1994). The present study, however, indicates that this assignment is unlikely owing to the high intensity of this band (Fig. 7) despite the low octahedral Mg content (Manceau et al. 2000a) of the unaltered Garfield nontronite. Russell et al. (1979) assigned it to a Si-O (apical)-stretching vibration, which could be visible by IR due to distortions in the tetrahedral sheet. However, Keeling et al. (2000) reported a $(Fe^{3+})_2(OH)$-libration band near 845 cm^{-1} for two hydrothermal nontronite samples.

The 790 cm^{-1} band was assigned to $Fe^{3+}MgOH$ deformation by Farmer (1974) and Goodman et al. (1976). However, this assignment is unlikely because the Garfield nontronite contains only 0.04 Mg cations per formula unit (Manceau et al. 2000a) whereas the 790 cm^{-1} band is relatively intense compared to the 822 cm^{-1} band. An alternative assignment for the 790 cm^{-1} band could be the Si-O vibration of an Si-rich admixture, such as amorphous silica, which absorbs near 790 cm^{-1}. Although a special method was used for the clay purification, this hypothesis remains viable, as the presence of such an amorphous phase is possible and its absence has yet to be proven. The assignment of the 589 cm^{-1} band is uncertain but it may be due to a combined Si-O-Fe^{3+}-bending mode (Stubican and Roy 1961a).

After 10 min of reduction, the 844 and 790 cm^{-1} bands both were lost (Fig. 7). The 822 cm^{-1} band shifted down to 814 cm^{-1} and remained close to that position for all levels of reduction. In addition, its intensity steadily decreased as reduction time increased. The 790 cm^{-1} band possibly shifted toward the main 822 cm^{-1} band, accounting for the shift of the latter to lower wavenumber. After 240 min of reduction, the 870 and 822–814 cm^{-1} bands also disappeared completely and a new band emerged at 653 cm^{-1}. No apparent connection was observed between this new band and any of the disappearing ones. However, a band located in the same region is generally observed for $(Fe^{2+})_3OH$-deformation modes in talc (Wilkins and Ito 1976). Thus, the 653 cm^{-1} band of the 240 min reduced Garfield nontronite could be due to $(Fe^{2+})_3OH$ deformation, which supports the hypothesis of trioctahedral domain formation upon reduction. However, the high intensity of this band suggests that it is not due only to $(Fe^{2+})_3OH$ deformation. A band located at 672 cm^{-1} for the unaltered Garfield nontronite does not change significantly upon reduction and could still be present in the spectrum of the 240 min reduced sample. The 653 cm^{-1} band observed for this sample could be generated by the overlap of one band at 672 cm^{-1} and another one due to $(Fe^{2+})_3OH$ deformation at lower wavenumber. The 672 cm^{-1} band is attributed to Fe-O out-of-plane vibration (Farmer 1974). This band is expected to shift to lower wavenumber upon Fe^{3+} reduction, but no evidence of such a shift was observed in the present study. The 589 cm^{-1} band decreased in intensity until it disappeared completely after 60 min of reduction.

The overall decrease in intensity of the M-Fe-OH-deformation bands upon reduction reflects once more the progressive loss of OH groups. The varying positions of these bands upon reduction are generated by changes in the cationic environment surrounding the remaining OH groups as more Fe^{3+} is reduced to Fe^{2+}.

The effect of reoxidation on M-Fe-OH deformations is illustrated by comparing the unaltered, reduced, and reduced-reoxidized samples together (Fig. 8). None of the spectra of the reoxidized samples is identical to that of the unaltered Garfield nontronite. Thus, reoxidation failed to restore completely the changes that occurred during Fe^{3+} reduction to Fe^{2+}, regardless of reduction time. However, the 822, 844, and 589 cm^{-1} bands were partially restored in all of the reoxidized samples, but the 844 and 589 cm^{-1} bands were missing from the 240 min reduced sample (Fig. 8d) after reoxidation. A connection was observed between the 844 and 589 cm^{-1} bands as these two bands were restored simultaneously. This connection tends to confirm the hypothesis that the 589 cm^{-1} band is due to a combined Si-O-Fe^{3+}–bending mode. The new band observed at 653 cm^{-1} in the 240-min reduced sample (Figs. 7 and 8d) disappeared upon reoxidation. This result agrees with its assignment to $(Fe^{2+})_3OH$-deformation modes, as almost all the structural Fe^{2+} was reoxidized (Table 1). If any changes in the 672 cm^{-1} band occurred upon reduction, they were completely restored upon reoxidation.

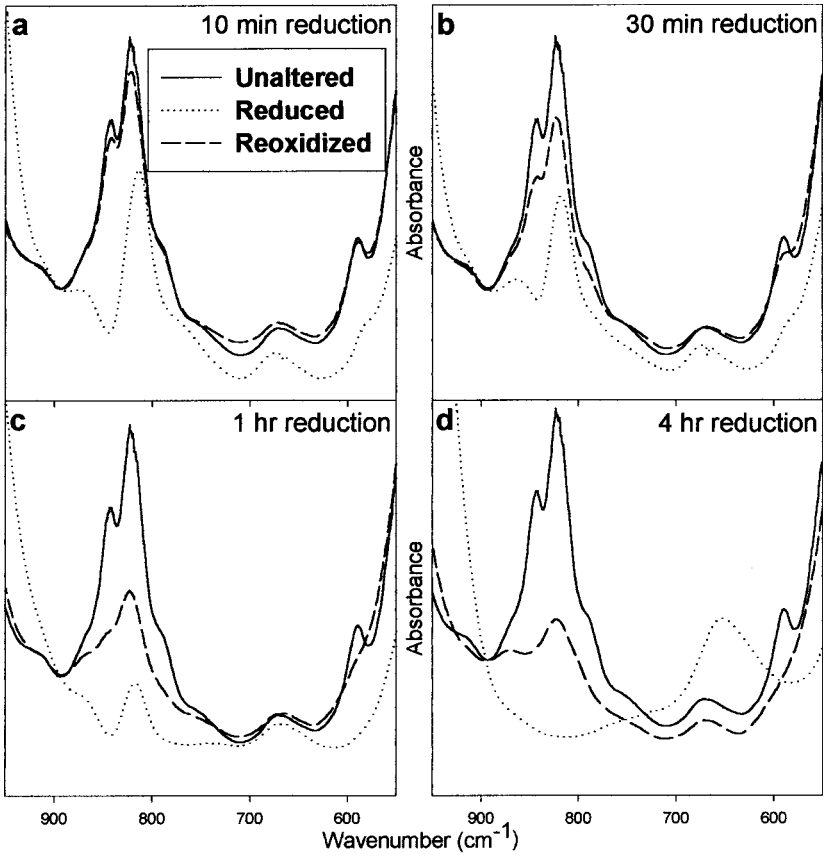

FIGURE 8. Normalized infrared spectra in the OH-deformation region of the Garfield nontronite reduced during different times, then reoxidized: reduction times of (**a**) 10 min; (**b**) 30 min; (**c**) 60 min; and (**d**) 240 min. The spectrum of the initially unaltered Garfield is given in each plot for comparison.

Si-O stretching: 800–1300 cm^{-1} IR Region

The Si-O-stretching band in the unaltered Garfield nontronite consists of the overlapping of two components in the range 1070–1110 cm^{-1} and two others at ~1034 and ~1000 cm^{-1} (Yan and Stucki 2000). The 1034 cm^{-1} component is an out-of-plane Si-O vibration whereas the three others are due to in-plane vibrations (e.g., Yan and Stucki 2000). The position of the intense Si-O-stretching band (Fig. 9) shifts progressively from 1029 cm^{-1} in the unaltered Garfield nontronite (0 min reduction time) down to 986 cm^{-1} after 240 min of reduction. A similar shift was observed by Yan and Stucki (2000), who found that the extent of shift in these bands affects the coupling between adsorbed water and the surface. Former studies showed that the Si-O-stretching band is shifted to lower wavenumbers upon layer charge increase and to higher wavenumbers upon charge decrease (i.e., Madejová et al. 1996; Komadel et al. 1999). Thus, the shift of the Garfield nontronite Si-O-stretching band upon reduction is at least partly due to the inherent charge increase. However, as already emphasized by Yan and Stucki (2000), this large shift could also result from the migration of some Fe atoms from *cis*- to *trans*-sites and the formation of trioctahedral domains.

Reoxidation of the reduced samples moved the Si-O band

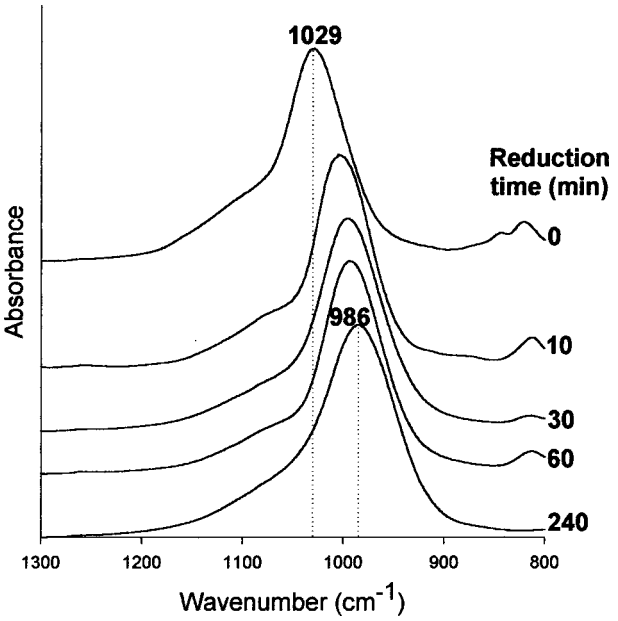

FIGURE 9. Infrared spectra in the Si-O-stretching region of the initially unaltered Garfield nontronite and of the samples reduced during 10 to 240 min with buffered sodium dithionite.

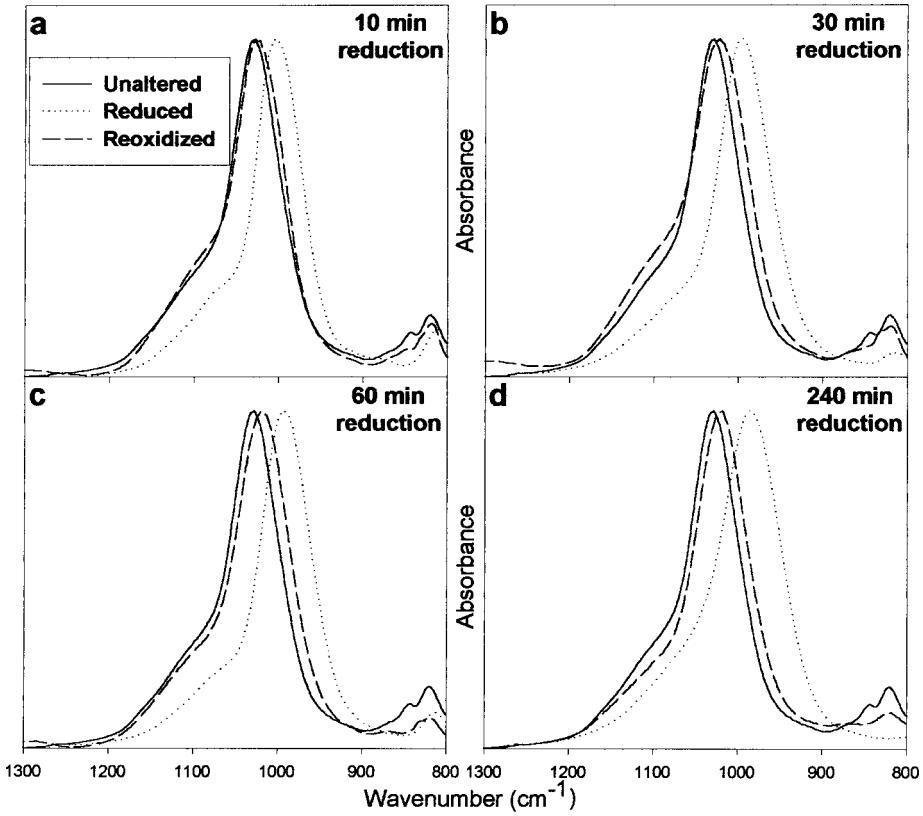

FIGURE 10. Infrared spectra in the Si-O-stretching region of the Garfield nontronite reduced during different times, then reoxidized: reduction times of (**a**) 10 min; (**b**) 30 min; (**c**) 60 min; and (**d**) 240 min. The spectrum of the initially unaltered Garfield nontronite is given in each plot for comparison.

(Fig. 10) in the direction toward, but not completely to, the original value (i.e., 1029 cm^{-1}) as already observed by Yan and Stucki (2000). For example, a difference of 10 cm^{-1} in the Si-O band position was observed between the unaltered Garfield nontronite (1029 cm^{-1}) and the sample reoxidized after 240 min of reduction (1019 cm^{-1}, Fig. 10d).

This remarkable change in Si-O wavenumber due to Fe oxidation state strongly refutes the previously accepted rule that the octahedral cationic composition has little effect on the Si-O wavenumber (Stubican and Roy 1961a). One could argue that the possible dissolution of Al in the medium of citrate-bicarbonate buffer could be responsible for the variations in Si-O wavenumber (Stucki et al. 1984b; Jackson 1979), but reoxidation substantially reversed the wavenumber shifts, which could not happen if the shift were due to dissolution. This finding clearly indicates that dissolution is unlikely to be the dominant process causing wavenumber shifts of the Si-O bands in the present study. Furthermore, the partial irreversibility of the Si-O band shift, even though the Fe^{2+} is virtually totally reoxidizable, indicates that factors in addition to changes in the layer charge affect the Si-O band position. Cation rearrangement along with changes in Fe oxidation state must be key factors affecting the Si-O stretching energy during reduction.

Proposed reduction sequence and irreversibility

During the first 10 min of reduction, only a change in Fe oxidation state and a superficial dehydroxylation occur, these changes being virtually reversible. As the reduction proceeds further, the loss of structural OH becomes more extensive and less reversible. As many as two OH groups are lost either simultaneously or sequentially from a given *cis*-hydroxide octahedron, forming strongly bound structural H_2O and significant cationic rearrangements in the octahedral sheet. The extent of irreversibility in this regard becomes increasingly evident as the initial level of reduction increases (Figs. 6b, 6c, 6d, 8b, 8c, 8d, 10b, 10c, and 10d). As the level of reduction increases, rearrangement of cations occurs to form trioctahedral domains. Upon reoxidation, cations are re-distributed in a different manner than existed in the unaltered clay, and the lost OH is only partially restored. The overall redox process is, therefore, in some respects irreversible even though virtually all Fe^{2+} in the structure can be reoxidized.

ACKNOWLEDGMENTS

The authors gratefully acknowledge financial support for this work from the USDA National Research Initiative Program (Grant 93-37102-8957), DOE-NABIR Program (Grant DE-FG01-00ER62986), and NSF Petrology and Geochemistry Program (Grant EAR-0126308).

REFERENCES CITED

Angell, C.L. and Schaffer, P.C. (1965) Infrared spectroscopic investigations of zeolites and adsorbed molecules. I. Structural OH groups. Journal of Physical Chemistry, 65, 3463-3470.

Besson, G., Bookin, A.S., Dainyak, L.G., Rautureau, M., Tsipursky, S.I., Tchoubar, C., and Drits, V.A. (1983) Use of diffraction and Mössbauer methods for the structural and crystallo-chemical characterization of nontronites. Journal of Applied Crystallography, 16, 374–383.

Burns, R.G. and Strens, R.G.J. (1966) Infrared study of the hydroxyl bands in clinoamphiboles. Science, 153, 890–892.

Cardille, C.M. (1987) Structural studies of montmorillonites by ^{57}Fe Mössbauer spectroscopy. Clay Minerals, 22, 387–394.

Caspers, H.H. and Buchanan, R.A. (1962) Crystalline field effect on OH^- in LiOH, $Ca(OH)_2$ and $Mg(OH)_2$. Spectrochimica Acta, 18, 1361.

Cracium, C. (1984) Influence of the Fe^{3+} for Al^{3+} octahedral substitutions on the IR spectra of montmorillonite minerals. Spectroscopy Letters, 17, 579–590.

Drits, V.A. and Manceau, A. (2000) A model for the mechanism of Fe^{3+} to Fe^{2+} reduction in dioctahedral smectites. Clays and Clay Minerals, 48, 185–195.

Drits, V.A. and McCarty, D.K. (1996) The nature of diffraction effects from illite and illite-smectite consisting of interstratified *trans*-vacant and *cis*-vacant 2:1 layers: A semiquantitative technique for determination of layer-type content. American Mineralogist, 81, 852–863.

Farmer, V.C. (1971) The characterization of adsorption bands in clays by infrared spectroscopy. Soil Science, 112, 62–68.

———(1974) The IR spectra of minerals, 344 p. Mineralogical Society, London, U.K.

Farmer, V.C. and Russell, J.D. (1964) The infrared spectra of layer silicates. Spectrochimica Acta, 20, 1149–1173.

Goodman, B.A., Russell, J.D., Fraser, A.R., and Woodhams, F.W.D. (1976) A Mössbauer and IR spectroscopic study of the structure of nontronite. Clays and Clay Minerals, 24, 53–59.

Grauby, O., Petit, S., Decarreau, A., and Baronnet, A. (1994) The nontronite-saponite series: An experimental approach. European Journal of Mineralogy, 6, 99–112.

Huo, D. (1997) Infrared study of oxidized and reduced nontronite and Ca-K competition in the interlayer, 139 p. Ph.D. thesis, University of Illinois, Champaign-Urbana.

Jackson, M.L., Ed. (1979) Soil chemical analysis-Advanced course, ed. 2, 895 p. Madison, Wisconsin.

Keeling, J.L., Raven, M.D., and Gates, W.P. (2000) Geology and characterization of two hydrothermal nontronites from weathered metamorphic rocks at the Uley Graphite Mine, South Australia. Clays and Clay Minerals, 48, 537–548.

Komadel, P. and Stucki, J.W. (1988) Quantitative assay of minerals for Fe^{2+} and Fe^{3+} using 1,10-phenanthroline: III. A rapid photochemical method. Clays and Clay Minerals, 36, 379–381.

Komadel, P., Lear, P.R., and Stucki, J.W. (1990) Reduction and reoxidation of nontronite: extent of reduction and reaction rates. Clays and Clay Minerals, 38, 203–208.

Komadel, P., Madejova, J., and Stucki, J.W. (1995) Reduction and reoxidation of nontronite: questions of reversibility. Clays and Clay Minerals, 45, 105–110.

———(1999) Partial stabilization of Fe(II) in reduced ferruginous smectite by Li fixation. Clays and Clay Minerals, 47, 458–465.

Lear, P.R. and Stucki, J.W. (1985) Role of structural hydrogen in the reduction and reoxidation of Fe in nontronite. Clays and Clay Minerals, 33, 539–545.

———(1990) Magnetic properties and site occupancy of iron in nontronite. Clay Minerals, 25, 3–13.

Madejová, J., Bujdák, J., Gates, W.P., and Komadel, P. (1996) Preparation and infrared spectroscopic characterization of reduced-charge montmorillonite with various Li contents. Clay Minerals, 31, 233–241.

Manceau, A., Lanson, B., Drits, V.A., Chateigner, D., Gates, W.P., Wu, J., Huo, D., and Stucki, J.W. (2000a) Oxidation-reduction mechanism of iron in dioctahedral smectites. 1. Crystal chemistry of oxidized reference nontronites. American Mineralogist, 85, 133–152.

Manceau, A., Lanson, B., Drits, V.A., Chateigner, D., Wu, J., Huo, D., Gates, W.P., and Stucki, J.W. (2000b) Oxidation-reduction mechanism of iron in dioctahedral smectites. 2. Structural chemistry of reduced Garfield nontronites. American Mineralogist, 85, 153–172.

Petit, S., Prot, T., Decarreau, A., Mosser, C., and Toledo-Groke, M.C. (1992) Crystallochemical study of a population of particles in smectites from a lateritic weathering profile. Clays and Clay Minerals, 40, 436–445.

Roth, C.B. and Tullock, R.J. (1973) Deprotonation of nontronite resulting from chemical reduction of structural Fe^{3+}. In J.M. Serratosa and A. Sanchez, Eds., Proceedings of the International Clay Conference, p. 107–114. Division de Ciensas, Madrid.

Roth, C.B., Jackson, M.L., and Syers, J.K. (1969) Deferration effect on structural ferrous-ferric iron ratio and CEC of vermiculites and soils. Clays and Clay Minerals, 17, 253–264.

Rozenson, I. and Heller-Kallai, L. (1976a) Reduction and oxidation of Fe^{3+} in dioctahedral smectites. 1: reduction with hydrazine and dithionite. Clays and Clay Minerals, 24, 271–282.

———(1976b) Reduction and oxidation of Fe^{3+} in dioctahedral smectites. 2: reduction with sodium sulphide solutions. Clays and Clay Minerals, 24, 283–288.

Russell, J.D., Farmer, V.C., and Velde, B. (1970) Replacement of OH by OD in layer silicates, and identification of the vibrations of these groups in infrared spectra. Mineralogical Magazine, 37, 869–879.

Russell, J.D., Goodman, B.A., and Fraser, A.R. (1979) Infrared and Mössbauer studies of reduced nontronites. Clays and Clay Minerals, 27, 63–71.

Serratosa, J.M. (1960) Dehydration studies by I.R. spectroscopy. American Mineralogist, 45, 1101–1104.

Strens, R.G.J. (1974) The common chain, ribbon and ring silicates. In V.C. Farmer, Ed., The IR spectra of minerals, p. 305–330. Mineralogical Society, London.

Stubican, V. and Roy, R. (1961a) Isomorphous substitution and infra-red spectra of the layer lattice silicates. American Mineralogist, 46, 32–51.

———(1961b) A new approach to assignment of infra-red absorption bands in layer-structure silicates. Zeitschrift fur Kristallographie, 15, 200–214.

Stucki, J.W. (1981) The quantitative assay of minerals for Fe^{3+} and Fe^{2+} using 1,10-phenanthroline: II. A photochemical method. Soil Science Society of America Journal, 45, 638–641.

Stucki, J.W. and Roth, C.B. (1976) Interpretation of infrared spectra of oxidized and reduced nontronite. Clays and Clay Minerals, 24, 293–296.

———(1977) Oxidation-reduction mechanism for structural Fe in nontronite. Soil Science Society of America Journal, 41, 808–814.

Stucki, J.W., Bailey, G.W., and Gan, H. (1996) Oxidation-reduction mechanisms in iron-bearing phyllosilicates. Applied Clay Science, 10, 417–430.

Stucki, J.W., Golden, D.C., and Roth, C.B. (1984a) Preparation and handling of dithionite-reduced smectite suspensions. Clays and Clay Minerals, 32, 191–197.

———(1984b) Effects of reduction and reoxidation of structural Fe on the surface charge and dissolution of dioctahedral smectites. Clays and Clay Minerals, 32, 350–356.

Stucki, J.W., Low, P.F., Roth, C.B., and Golden, D.C. (1984c) Effects of oxidation state of octahedral Fe on clay swelling. Clays and Clay Minerals, 32, 357–362.

Stucki, J.W., Wu, J., Gan, H., Komadel, P., and Banin, A. (2000) Effects of iron oxidation state and organic cations on dioctahedral smectite hydration. Clays and Clay Minerals, 48, 290–298.

Wilkins, R.W.T. and Ito, J. (1976) Infrared spectra of some synthetic talcs. American Mineralogist, 52, 1649–1661.

Yan, L. and Stucki, J.W. (1999) Effects of structural Fe oxidation state on the coupling of interlayer water and structural Si-O stretching vibrations in montmorillonite. Langmuir, 15, 4648–4657.

———(2000) Structural perturbations in the solid-water interface of redox transformed nontronite. Journal of Colloid and Interface Science, 225, 429–439.

MANUSCRIPT RECEIVED DECEMBER 5, 2000
MANUSCRIPT ACCEPTED DECEMBER 14, 2001
MANUSCRIPT HANDLED BY ALAIN BARONNET